EFFECT OF NON-STRUCTURAL ELEMENTS ON THE OVERALL RESISTANCE OF A BUILDING

FINAL YEAR PROJECT UG-2018

By

Iman Sahibzada Jan

Ahmed Hammad Haider

Atif Ilyas Malik

Syed Muhammad Ali

Project Advisor

Dr. Sarmad Shakeel

NUST Institute of Civil Engineering

School of Civil and Environmental Engineering

National University of Sciences and Technology

Islamabad, Pakistan

2021

EFFECT OF NON-STRUCTURAL ELEMENTS ON THE OVERALL RESISTANCE OF A BUILDING

FINAL YEAR PROJECT UG-2018

By

Iman Sahibzada Jan (G.L)	- 241643
Ahmed Hammad Haider	- 246841
Atif Ilyas Malik	- 249659
Syed Muhammad Ali	- 266271

Project Advisor

Dr. Sarmad Shakeel

NUST Institute of Civil Engineering

School of Civil and Environmental Engineering

National University of Sciences and Technology, Islamabad, Pakistan

2021

APPROVAL SHEET

This is to certify that the contents and forms of the thesis titled “Effect of non-structural components on the structural resistance of a building” is the original work of the author(s) and has been carried out under my direct supervision. I also certify that the thesis has been prepared under my supervision according to the prescribed format and I endorse its evaluation for the award of a Bachelor of Civil Engineering Degree through the official procedures of the Institute.

Dr. Sarmad Shakeel

Assistant Professor (Project Supervisor)

NICE, SCEE, NUST

Dr. Muhammad Usman

HOD Structures

NICE, SCEE, NUST

Dean / Principle

NICE, SCEE, NUST

ACKNOWLEDGEMENTS

Praise be to Allah SWT for giving us the knowledge and strength to complete this research. We would like to thank our advisor Dr. Sarmaad for guiding us every step of the way in our project and dedicating his precious time to our group. Also, providing us with equipment to help complete this research. And we would like to acknowledge the positive attitude of our classmates towards our project that helped us push through hurdles. And lastly, we would like to thank our parents for their constant support throughout this project and for blessing us with this opportunity to study at such a prestigious university.

ABSTRACT

Full-scale experimental checks and corresponding modeling efforts by way of researchers have revealed that, even though the structures designed in line with current seismic requirements maintain the MCE stage earthquake shaking, there may be a high degree of in-determinism in reaction and conservatism within the layout. This is obtrusive from the consequences of shake table assessments, wherein the structure is supposed to undergo intense damage as in line with the design recommendations, however simplest superficial damages occur. This indeterminism/redundancy is delivered using the contribution of “so-referred to as” non-structural partition walls and cladding to the structural response at the system level. This paper investigates this impact by designing and modeling CFS buildings at numerous proportions of non-structural wall panels. A simplified model incorporating a zero-length spring element is generated in OpenSees. The response of a building to lateral loading without and with facades was compared by performing a pushover analysis. The results determined that incorporating facades increases the stiffness of the building and prolongs its behavior in the linear range.

TABLE OF CONTENTS

LIST OF TABLES

LIST OF FIGURES

CHAPTER ONE

1. INTRODUCTION

1.1 Background

1.1.1 Difference between Structural and Non-Structural Components

Most of the modern buildings have two major components which can be broadly classified into two categories i. structural components ii. Non-structural components. The structural components compromise foundation, beams, columns, load-bearing walls, and roof slabs. Whereas the non-structural components comprise partition walls and infilled façades. Partition walls and infilled façades are non-load bearing walls. They do not carry the load of ceiling or floor above them rather they are designed only to carry their own material load.

1.1.2 Difference between Infilled Façades and Partition Walls

Infilled façades are also partition walls. The only difference between infilled façades and partition walls is that infilled façades are used on the outer side of the building. Being exposed to the weathering elements infilled façades mostly has extra protective layering.

1.1.3 Materials for Construction of Infilled Façades and Partition Walls

Partition walls and infilled façades can be made from different materials. Depending upon their material they can have different properties. However, whatever the material they may be made of they have a common purpose which is to provide privacy and insulation. The most common types of partition walls and infilled façades based on the material are brick masonry, concrete, wooden, straw board and light gauge steel (LGS) partition walls. For our research work, we will be focusing on LGS partition walls and infilled façades and particularly on LGS infilled façades as the these are most common type of partition walls used in steel buildings These partition walls are infilled façades have a basic frame that is made of LGS which is then filled with insulating material like gypsum boards.

1.2 Introduction of LGS Façades and Partition Walls

1.2.1 Introduction of Light-Gauge Steel (LGS)

Light-gauge steel is actually cold-formed or cold-rolled steel. The construction process using LGS sections is similar to the wooden framing construction. These sections are usually coated with zinc to protect them against corrosion. LGS sections are both used for structural and non-structural framing. The reason it is called light gauge steel is because of the thickness of its sections. For the structural section, their thickness ranges from 1-3mm while for non-structural members their thickness ranges from 0.6-1mm. Some benefits which LGS sections have over conventional steel and wood framing are like having strong strength-to-weight ratio, easy relocation and repair, and better fire performance, especially when compared to wooden framing.

1.2.2 Layout of LGS Partition Walls and Façades

Coming towards the basic layout of LGS partition walls and infilled façades, they have one thing in common which is the LGS frame. This LGS frame is made of horizontal members called tracks and vertical members called studs. These tracks and studs are joined together by screw connections or by punched connections. The tracks are made U-shaped so the tracks can be fit inside the flange of the tracks making a secure connection. This also allows using screws only on the top track to fix the studs in their place. The studs are placed between the two tracks at a particular interval. The frames are can be fixed from all sides or only from sides to structural members by use of the screws. These frames are then filled with gypsum boards and insulating materials. In the case of infilled façades, they have cemented boards with cement-based plaster on the outer side which protects the infilled façades from weathering elements.

1.3 Problem Statement

1.3.1 Research Gap

Structural members like beams, columns, and shear walls are very important for the stability of the whole building. Therefore, great care is taken while designing these structural members of the buildings. And usually they are overdesigned against the expected earthquake loading. But that's not the case for parathion walls and façades. Since these infilled partition walls and façades do not have to carry any structural load, they were not designed as thoroughly as the structural members. And over the years this has led to a research gap. Although these infilled façades and partition walls are not carrying any structural load they are connected to the structural members through a fixed connection. Therefore, in case of earthquake loading these infilled façades and partition walls also undergo seismic loading. In cases where these partition walls and infilled façades are not designed properly, they may undergo partial or complete failure.

1.3.2 Importance of Filling Research Gap

Although the failure of these infilled façades or partition walls does not cause a catastrophic failure of the building, damage to these can cause significant financial costs needed to repair or completely replace the partition wall. Also failure of these members affects the functionality of the building. In addition to this, falling components of failing façades can also injure people standing below them. All of these concerns demand through studies of seismic response and failure mechanism of the infilled facades and partition walls.

1.3.3 Challenges in Research

In the past studies have been carried out to determine the seismic response of these infilled façades and partition walls but the number of these studies is small. In addition to that, most of these studies were based on the experimentation with individual façades and partition walls. The seismic response of these infilled facades and partition walls is still not fully understood. The major hindrance in this regard was the complexity of the project need to be carried out to study their effect. As construction of a whole building just for research purposes is not an easy task.

1.4 Research Objectives

Our research work aimed to understand the behavior of infilled façade and partition walls under seismic loading, and study their failure mechanism. Then using our analysis, provide the best façade configuration which performs well against seismic loading. Another important aim of our study was to study the effect of these infilled facades to the seismic performance of the building. For this purpose, numerical model of a steel building and as well as LGS façades were developed in OpenSees software. The building models and LGS façades models were then incorporated together and seismic analyses were performed. The results obtained from these analyses were used to determine the effect of the LGS façades on the seismic performance of the building.

2. Literature Review

2.1 LGS Infilled Walls as Façades and Partition Walls

Cold-formed Light Gauge Steel (LGS) walls are the most commonly used non-structural walls used as façades and partition walls [Jose´ I. Restrepo et al. 2011; Ali Sahin Tasligedik et al. 2014]. The non-structural elements are mostly not designed to carry vertical or lateral loads other than their self-weight. But these LGS walls are mostly connected to the load-carrying members at multiple locations. During the event of an earthquake, these LGS walls undergo excitation imposed by the structure. As a result, the damage in these elements is associated with inter-story drift drifts and deflections of the primary structure. [ASCE 7-10] recommends the wall connections should be designed with adequate deformability to account for the variation in displacement. However, the introduction of deformability designs in the industry is a very challenging task. The reason is not only because of their complex geometric configuration but also due to the lack of studies investigating the force-deformation behavior of these LGS elements under seismic loading. Only a few studies are available in the literature which can be used for the calibration of models of LGS partition walls for seismic analysis. The most relevant work done in this regard was by [Restrepo and Bersofsky. 2014]. Similar work was done by Japanese researchers [Lee et al. 2006]. The main difference between the work of [Restrepo and Bersofsky. 2014] and [Lee et al. 2006] is that the latter didn't use the top tracks in their models.

2.2 Damages to LGS Infilled Façade and Partition Walls

Cases from the past earthquake have shown severe damage to these LGS walls. Damages such as cracking of gypsum boards, bending of studs, failure of connections between track and slab, and partial/complete failure of infilled façades and partition walls were reported during these earthquakes [Craig Jenkins et al. 2016]. Damage to these LGS walls is a major concern as failing partition walls and façades not only cause economic losses [Miranda et al. 2012; Baird et al. 2014] but the falling components from these partition walls and façades can also injure the people below. The majority of the earthquake damages are to the non-structural infilled façades and partition walls [Craig Jenkins et al. 2016]. The buildings may be structurally intact after an earthquake event but the damaged/failed infilled façades and partition walls can make their immediate occupancy impossible. The functionality of strategic buildings is very critical after an earthquake event making the seismic behavior of non-structural components very crucial to be considered [De Stefano et al. 2012].

2.3 Damage Propagation in LGS Infilled Façade and Partition Walls

Therefore to investigate the seismic behavior of the LGS walls and to use these findings in engineering practice several studies have been undertaken. For example, [McMullin and Merrick. 2005] and [Rihal SS. 1987] investigated the damage propagation of LGS partition walls but they didn't consider any specimen mounted on the structural frame. [Lee et al. 2006] investigated the seismic performance of LGS partition walls used in Japanese industry. They developed the full-scale models of partition walls mounted on the structural frame. Using the quasi-static loading they assessed the damage against the structural response like inter-story drift. [Restrepo and Bersofsky. 20007] studied the behavior of 16 CFS partition wall specimens under quasi-static loading. [Lang, A. F., and Restrepo, J. I. 2007] were the first to present the seismic damage metrics for the partition walls subjected to quasi-static cyclic loading.

2.4 Quasi-Static Raking Testing of LGS partition Walls

[Restrepo and M. Bersofsky 2010] performed quasi-static raking testing on LGS partition walls with gypsum boards. Eight identical LGS partition wall specimens were tested with variables like stud thickness, stud spacing, spacing of self-tapping screws, and wallboard thickness. Based on the results they presented the in-plane seismic performance characteristics of the LGS partition walls. Also they observed different limit states in partition walls. Based upon their observation these limit states were divided into three groups of Damage States. These damage sates were related to the inter-story drift ratios. Damage State I occurred at 0.05-1% inter-story drift ratio required minor repairs if needed. Damage State occurred at 0.5-1.5% inter-story drift requiring repairs which may interrupt usual business, Damage State I occurred at 0.5-3% inter-story drift ratio requiring complete change of partition wall. [Davies et al. 2011] studied the fragility of the walls under in-plane simulated seismic loading. They used numerical models to study the in-plane seismic response of full-scale LGS partition walls. Experimental data was used to develop a numerical model using the System for Earthquake Engineering Simulation (OpenSees) modeling platform. To capture the non-hysteretic response of the LGS partition walls, a lumped material was developed using the pinching 4 material available in OpenSees.

2.5 Full Scale Building Testing

While competent level studies have been performed by many researchers. Only a few tests have been performed on full-scale building levels. Full-scale building tests are very important as they allow to study of the interaction between the walls and primary structure. Also, they provide an opportunity to study the interaction between these walls and other non-structural components. A few examples of system-level tests performed are [Restrepo and Lang 2011; Sasaki et al. 2012]. Also, most of the studies were done for the interior partition walls and only a few studies are available that investigate the exterior LGS façade performance against the seismic loadings. Some examples of these studies are [Nakata et al. 2012; Schafer 2013].

[Gennaro et al. 2013] performed the shake table testing of plaster board-based LGS partition walls to evaluate their performance against the seismic loading. A full-scale story model LGS partition was developed and tested in both horizontal directions with eleven different shaking intensities to investigate seismic damages and various inter-story drift demands. [R. Retamales et al. 2013] carried out an experimental program to study the seismic response and fragilities of gypsum board-based LGS partition walls. For this study, in-plane quasi-static and dynamic testing was performed on 36 LGS partition wall specimens with 16 different configurations. Effects of variables like stud connection type, framing thickness, and partial wall height were studied through these 16 configurations.

[X. Wang et al. 2015] performed the shake table testing of the full-scale five-story building. The study was done to see the performance of LGS partition walls and façades against seismic loading and to see their interaction with the primary structure and structural elements. The experiment studied the relationship between the drift demands of building with the damaged state of partition walls.

2.6 Damage Assessment Testing

[Tasligedik AS, Pampanin S. 2015] performed the damage assessment of LGS partition walls and then proposed design modifications for existing walls to increase their tolerance to damage caused by inter-story drift. The study found that LGS frames of partition walls, constructed using US and NZ industry practices, will lose serviceability at 0.3% inter-story drift. Based upon the observation they presented low damage solutions. By introducing design modifications like letting the studs and lining slide inside the LGS track they delayed the occurrence of cracks at the lining interface. [Petrone C, Magliulo G. 2015] reported the damage assessed during in-plane quasi-static loading of plasterboard LGS partition walls.

2.7 Effect of Supplementing Adhesives

[Swensen S, Deierlein GG 2016] studied the seismic behavior of LGS partition having screws or adhesive connection between the gypsum wallboard and LGS frame. For the experiment enhanced screw connections were developed and were compared with connections with conventional screws as well as with construction adhesives. The tests showed that the stiffness and strength of conventional connections can be increased up to four times by supplementing them with adhesives.

2.8 Story Level Testing on Shake Table

[Jenkins. C, Soroushian. S 2016] presented the study on seismic performance of drift-sensitive nonstructural systems. The results of this study were based on the seismic analysis of a full-scale, two-story, one-bay braced frame structure. The seismic loading was applied through biaxial shake tables. The performance of LGS frames was evaluated using design variables like (1) partition wall geometries, (2) framing systems type, (3) connection types, and (4) opening in partition walls. The performance evaluation of top connections, out-of-plane acceleration amplification factors, and fragility curves based on damage caused by inter-story drift was among the experimental outcomes.

Even after these studies and experimental programs, there is still an obvious gap in knowledge and understanding of the seismic behavior of the LGS-infilled façades and partition walls. To fill this gap a series of experimental programs and research projects were initiated in the Department of Structures for Engineering and Architecture of the University of Naples "Federico II. The main focus of these studies was to investigate and comprehend the seismic response of non-structural façades, partition walls, and suspended ceilings. These projects covered different aspects like material testing [Fiorino L, Masello V, et al. 2017], in-plane and out-of-plane [Fiorino L, Herfurth D, et al. 2015; Pali T, Macillo V 2018] testing of façades and partition walls [Fiorino L, Macillo V, et al. 2017].

2.9. LGS Partition Walls Surround by RCC Structural Members

In the study [Tatiana Pali et al. 2018] the seismic behavior of partition walls surrounded by RCC structural members from all sides, was observed. For comparison the partition walls connected to beams or floor from top and bottom, having connections with transverse façades at their ends were also tested. The study aimed to study the seismic behavior of partition walls while incorporating the effect of the surrounding structural members as well as non-structural elements like outdoor façades. During the study effects of constructive parameters like fixed or sliding connections and sheathing panel types were investigated to find the effect of lateral response in secant stiffness in the case of quasi-static reversed cyclic loading. It was found that the specimens with sliding connections showed same level of damages as in with fixed connections, at a higher inter-story drift ratio. Making sliding connections more advantageous in case of seismic vulnerability.

2.10. Assessment of Local Behavior and Response to Quasi-Static Loading

[Tatiana Pali and Sarmad Shakeel. 2019] presented their study based on the seismic performance evaluation of LGS non-structural components. The study was backed by experiments on several LGS framed non-structural components like indoor partition walls, façades, and suspended continuously suspended ceilings having gypsum or cement infills. The tests were performed systematically starting from the ancillary level, then element level tests, and finally assembly-level tests. These test series assed the local behavior, response to quasi-static loading, and dynamic behavior of these LGS non-structural components. Main findings of this study showed that stud spacing greatly influence the characteristics of partition walls like stiffness, strength and fundamental vibrational frequency.

Even though experiments were performed by researchers and computational models are being developed there is still a need for more studies for defining the seismic objectives necessary for LGS walls in future seismic design codes. To tackle this need [Sarmad Shakeel et al. 2019] compared the seismic fragility evaluation of LGS partition walls with those already present in the literature. This was done to study damage progression which was further used for the identification of damage type and for studying their association with different damage states.

2.11. Summary

The present studies are mainly based on experimental work and extensive shake table testing. Similarly, most of the previous studies discuss results that were derived from the shake table testing of individual LGS façades and partition walls. Few studies are available where the seismic response of the LGS partition walls and façades was studied on a story level and most of those experimental setups were having RCC members around the partition walls and façades and even fewer studies are present where the seismic performance of LGS non-structural components is evaluated on a full-scale building level. The reason behind this is the fact that performing these experiments on a building level is challenging and complex. In recent years' computational models are being developed of individual models, on platforms like OpenSees. This study aims to use the previous models and experimental data as reference and construct the building as well as infilled façades model. These façades and building models will then be used to study the effect and contribution of the LGS\façades to the seismic performance of the whole building.

3. METHODOLOGY

3.1. Description of Modeled Facades

The basic component of any Infilled Light Gauge Steel Façade is its frame. The frame is made of thin sections of galvanized steel sheets cold formed to make sections. The sections include studs, tracks, U-channels, and L-Headers. Studs are used for the vertical elements of the wall system. Tracks are used as the top and bottom plate of a wall for the studs to attach to. U-channel has multiple uses but all are related to wall reinforcement. Finally, the L-Header which is an L-shaped piece used for the assembly of headers.

These sections are called Light-Gauge because of their thickness. Their thickness ranges from 0.6 to 1mm. The sections are connected together by screwed or punched connections.

The Interior of the frame is filled with standard gypsum boards, impact-resistant gypsum boards, and insulating boards. In the case of the façade, it can be covered with cement-based plaster to protect it from weather elements.

Figure 3.1: Infilled facades

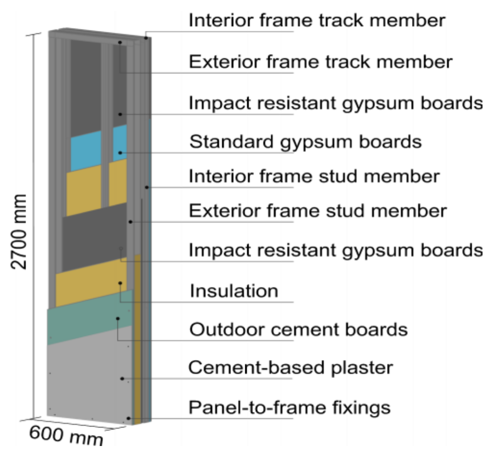

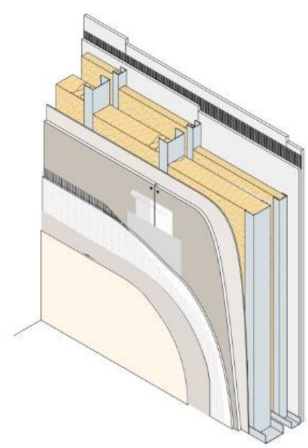

3.2. Façade Configuration

The following table shows the detailed differences of the 8 façade models that have been used in our study. We can see that none of the models have any offset. Also, model 1 is double framed while all the others are single framed structures. As far as the connections are concerned, model 6 has a sliding connection while all other models have fixed connections. More details are given as under.

Table 1: Façade configuration

Wall configuration No.	Wall frames properties: External Frame: Stud thickness (mm) 1	Stud spacing (mm)	Web height	Claddings Present	Internal Frame: Stud thickness (mm) 1	Stud spacing (mm)	Web height	Surroundings: Type of connection to surroundings 2	Off set	Panel properties: External Frame: Interior face	Exterior face	Internal Frame: Interior face	Exterior face
1 (BASIC)	0.6	600	75	No	0.6	600	50	Fixed	No	Diamant 12.5mm	Aquapanel 12.5mm	Not present	Diamant 12.5mm(outer) + Diamant 12.5mm(inner)
4	0.6	600	75	No				Fixed	No	Diamant 12.5mm	Aquapanel 12.5mm		
5					0.6	600	50	Fixed	No			Not present	Diamant 12.5mm(outer) + Diamant 12.5mm(inner)
6	0.6	600	75	No				Sliding	No	KB 12.5mr	Aquapanel 12.5mm		
7	1	600	150	Yes (Ω profile and				Fixed	No	KB 12.5mr	Aquapanel 12.5mm		
10					0.6	600	50	Fixed	No			Not present	GKB 12.5mm(outer) + GKB 12.5mm(inner)
18	1	600	150	No				Fixed	No	KB 12.5mr	Aquapanel 12.5mm		
20	0.6	600	75	No				Fixed	No	KB 12.5mr	Aquapanel 12.5mm		

For a better understanding of the differences in the configurations of our façade models, schematic diagrams are shown.

Test 1

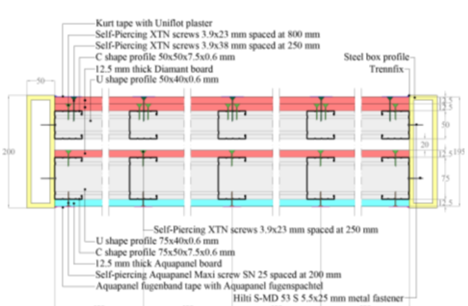

Test 5

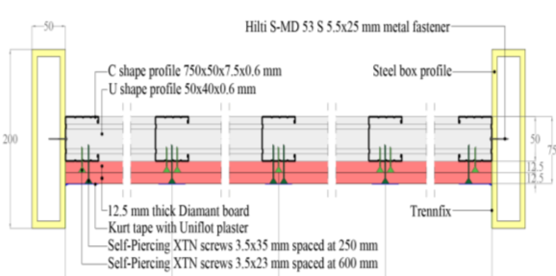

Test 4

Test 6

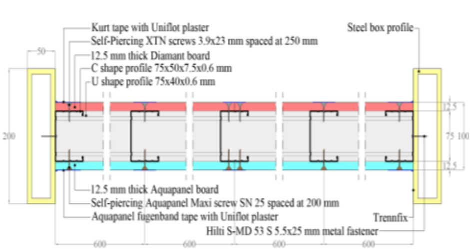

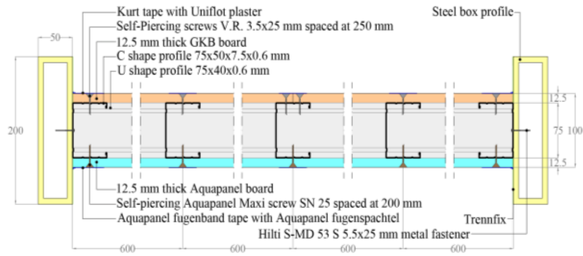

Test 7

Test 10

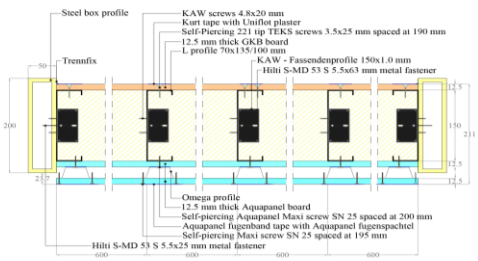

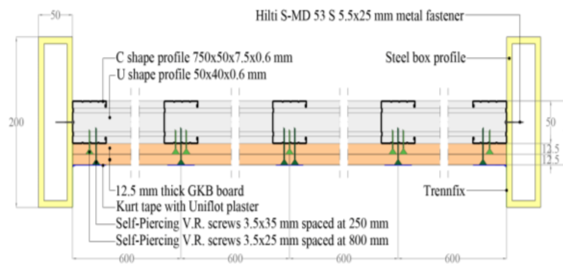

Test 18

Test 20

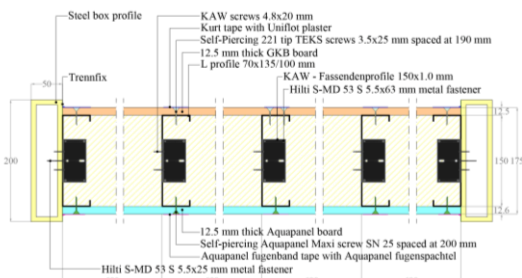

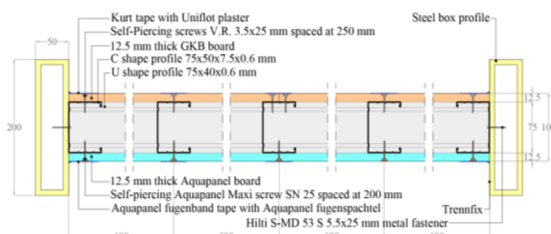

Figure 3.2: Façade configurations

3.3. Model Description

A zero-length spring element lumped with the global hysteretic behavior of the wall is developed in OpenSees [S. Mazzoni et al., 2009] software for all the 8 different tested façades. Firstly, a model for each of the individual facades is developed and then these models were grouped together into 5 groups on the basis of common characteristics which are defined in the previous section. The 5 groups developed are as follows

- **Group 1**: Dual frame (Test 1)
- **Group 2:** Sliding connection (Test 6)
- **Group 3:** Internal Frame only (Test 10, Test 5)
- **Group 4:** Stud thickness, Stud spacing and Web height **(**Test 7, Test18)
- **Group 5:** Stud thickness, Stud spacing and Web height **(**Test 4, Test 20)

For the zerolength spring element Pinching4 material has been used which is a uniaxial material which can represent the pinched load deformation and also the ability to exhibit degradation under cyclic loading. A set of 39 parameters are used to define the Pinching4 material. Out of these 39 parameters, 16 parameters are used to define the backbone curve (ePf1, ePd1, ePf2, ePd2, ePf3, ePd3, ePf4, ePd4, eNf1, eNd1, eNf2, eNd2, eNf3, eNd3, eNf4, eNd4), 5 parameters are used to define the cyclic behavior (uForceP, uForceN, rDispP, rDispN, rForceP, rForceN), 5 parameters for governing the strength degradation (gF1, gF2, gF3, gF4, gFLim), 5 parameters for controlling the unloading stiffness degradation (gK1, gK2, gK3, gK4, gKLim), 5 parameters for controlling the reloading stiffness degradation (gD1, gD2, gD3, gD4, gDLim), and 2 parameters for limiting the maximum degradation in each cycle (gE, dmgType).

For load transfer to the zerolength spring element, it is connected via 4 truss elements to the surrounding structural members ie beam and column. The beam and columns are pin connected and hinged at the base as shown in figure 3.3. The complete model has 3 degrees of freedom: the horizontal and vertical translations and the rotation in the plane of the wall

Figure 3.3: Model Schematic Diagram – Deformed Model shape

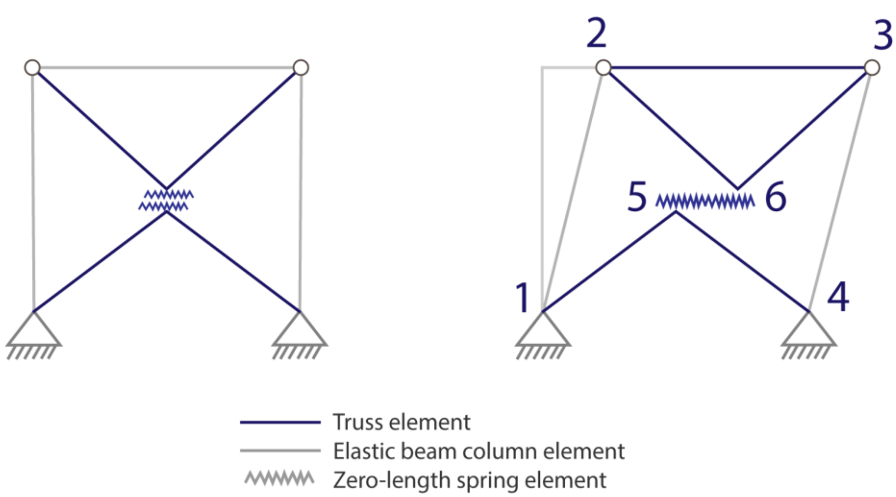

3.4. Test Setup

In the test setup (shown in Figure 3.4) the columns are modeled as BeamColumn element and the beam is modeled as truss element. The reason behind the usage of different elements for beam and column is due to the pin restraint being imposed twice, once due to the in-built pin restraint in truss element and twice due to the external pin restraint. Another option is to model both elements as BeamColumn element but that would require defining extra nodes at end of beam for release of bending moments. This alternative is not used to keep the model as simple as possible. The truss elements connecting the zerolength spring element have extra constraints at their end in order to ensure a proper load transfer to the zerolength spring element. The deformed shape of the model is shown in Figure 3.3.

Figure 3.4: Test Setup

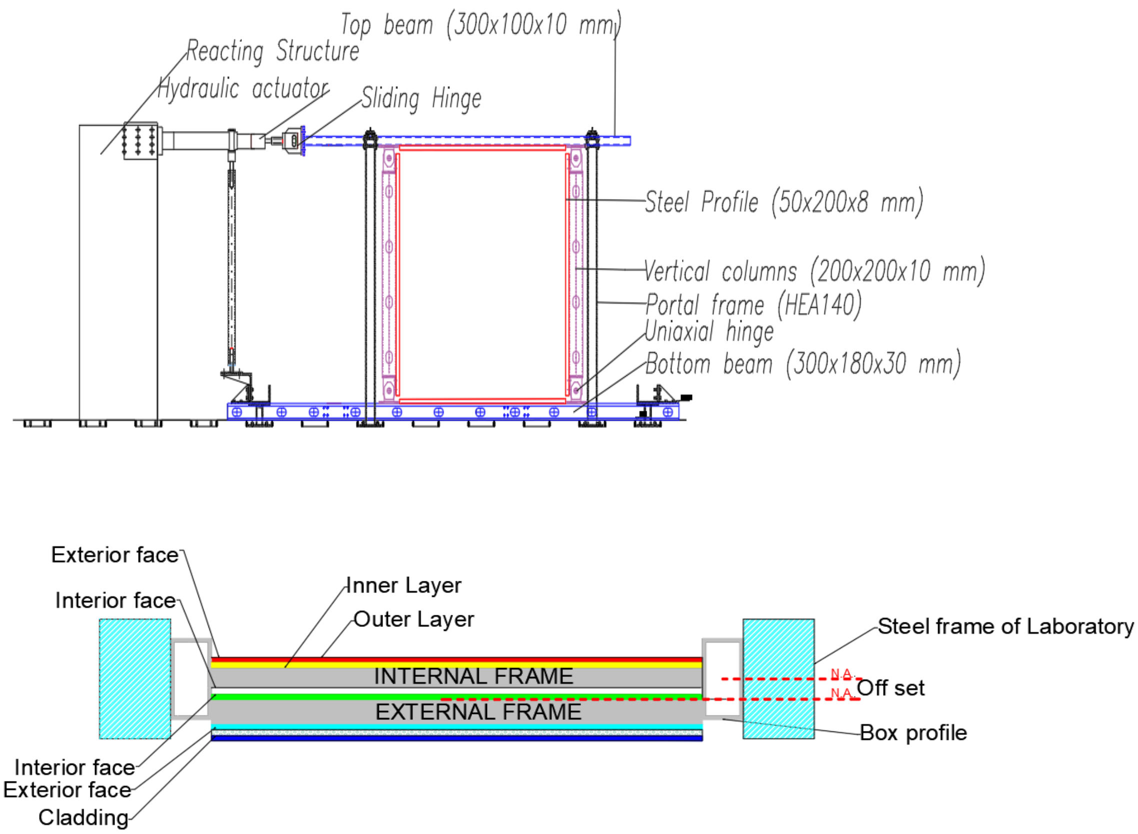

3.5. Individual Test Models

3.5.1. Hysteretic characterization

A four-point backbone curve of Pinching4 material is used to capture the envelope of experimental hysteretic response curve along with the strength degradation observed during the tests, after the wall had achieved its peak strength. The criteria (Figure 6) used to select the four points of the backbone curves, which were equal and opposite for the positive and negative directions of hysteretic envelope, are as follows:

- Point 1 (ePd1, ePf1): the force is calculated considering 20% of the peak force recorded during the test (Fp) while the displacement is the corresponding displacement at that point;

- Point 2 (ePd2, ePf2): the force is calculated considering 80% of the peak force and the displacement is chosen through an energy balance in such a way that the area below the experimental hysteretic envelope curve up to the peak point (A1) is equal to the area below the numerical backbone curve (A2) up to the peak point;
- Point 3 (ePd3, ePf3): the force is set equal to the peak force recorded during the test (Fp) while the displacement is the corresponding displacement at that point;
- Point 4: the force is calculated through an energy balance to have an equal area below the third and fourth points of the experimental hysteretic envelope curve (A3) and the numerical backbone curve (A4). The displacement (D*) is fixed at a value 3.5% of inter storey drift ratio (IDR) for the configurations having single partitions with fixed or sliding connections on top, 4.7% of IDR for the configurations having partitions connected on sides to the return walls while connected on top with fixed or sliding connections and 6.5% of IDR for the configurations having partitions with sliding connections on top and sides. The differences in IDR's for the configurations with and without sliding connections highlight the capability of sliding connections to accommodate higher drifts.

The unloading and reloading paths in hysteretic response curves are controlled by a series of parameters that govern the cyclic behavior. As regards to the positive branch, uForceP defines the ratio between the strength developed upon unloading and maximum strength of the positive backbone curve. rDisand rForceP mark the strength and displacement at which reloading occurs. Obviously, same definitions apply for negative branches (uForceN, rDispN, rForceN). As far as rDisis concerned, a best fit value is obtained by varying its value from 0.1 to 1.0 until a value is selected, with which minimum difference in the energy dissipated by the experimental and numerical results is obtained. Additionally, rest of the parameter were taken as zero, except in some cases, where a non-zero value is used for them to achieve a best fit. Table 2 list the values of cyclic parameters of Pinching4 material used for all tested configurations.

Table 2: Cyclic Loading Parameters Pinching4 Material

	ePF1	ePF2	ePF3	ePF4
	[KN]	[KN]	[KN]	[KN]
Test 1	9.229	36.9	46.1	19.2
Test 4	7.859	31.4374	39.296	13.02
Test 5	6.876	27.506	34.383	20.99
Test 6	5.34	21.367	26.71	14.662
Test 7	5.241	20.967	26.209	21.78
Test 10	4.28	17.119	21.399	14.034
Test 18	6.403	25.614	32.018	11.555
Test 20	6.093	24.371	30.464	23.909

ePd1	ePd2	ePd3	ePd4
[mm]	[mm]	[mm]	[mm]
3.5	11.6	27.8	70.0
3	13.65	25.3	81
2.664	21.375	40.06	81.2
2.08	15.09	77.2	125
1.36	15.66	27.65	106
1.12	8.97	78.5	105.1
2.3	15.43	28.3	57
1.74	5.945	105.75	130

	eNF1	eNF2	eNF3	eNF4
	[KN]	[KN]	[KN]	[KN]
Test 1	-9.228	-36.915	-46.143	-19.2
Test 4	-7.5896	-31.438	-39.298	-13.02
Test 5	-6.876	-27.504	-34.38	-20.92
Test 6	-5.34	-21.36	-26.71	-14.66
Test 7	-5.241	-20.996	-26.208	-21.708
Test 10	-4.28	-17.119	-21.399	-14.034
Test 18	-6.403	-25.613	-32.017	-11.556
Test 20	-6.093	-24.371	-30.464	-23.909

eNd1	eNd2	eNd3	eNd4
[mm]	[mm]	[mm]	[mm]
-3.5	-11.59	-27.8	-70
-2.5	-14.15	-25.3	-81
-2.66	-21.24	-40	-81.2
-2	-15.17	-77.2	-125
-1.25	-15.77	-27.65	-106
-1.12	-8.97	-78.5	-105.1
-2.4	-15.3	-28.3	-57
-1.74	-5.945	-105.75	-130

3.5.2. Model validation

The same cyclic loading protocol as used in the tests [Pali et al., 2018] has been used to analyze the model. This loading protocol has been defined by FEMA 461 [FEMA, 2007]. "Interim testing protocols for determining the seismic performance characteristic of structural and non-structural components". FEMA 461 provides a loading history that consists of repeated cycles of step-wise increasing deformation amplitudes. A comparison of different façade configurations in terms of hysteretic response is also shown in the figure 3.5.2.1.

Figure 3.5.2.1: Loading Protocol used in tests

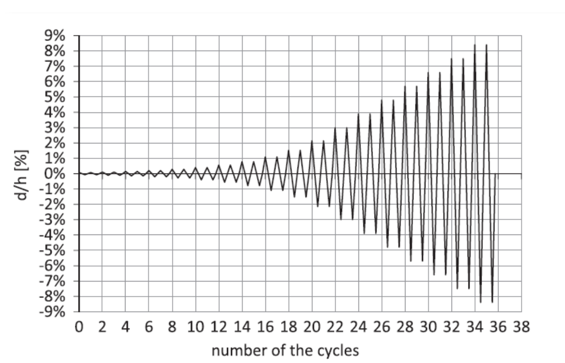

Test 6

Test 20

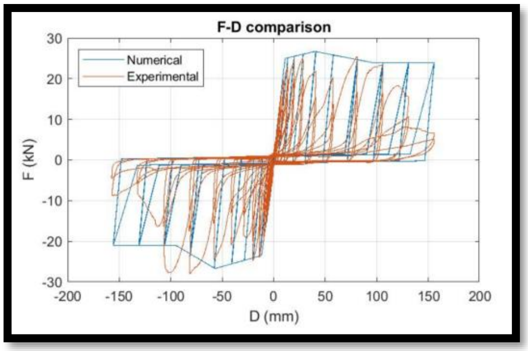

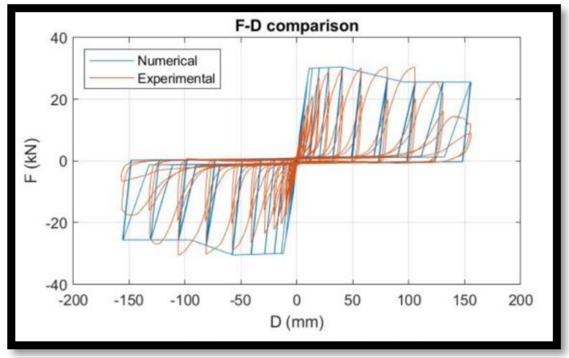

Figure 3.5.2.2 : F-D response comparison

It can be clearly seen that the numerical model effectively captures the F-D response of the tested façade configurations, both in terms of the peak points and the overall shape of the response. A comparison of cumulative energy dissipation of different façade configurations is shown in the figure below

Test 6

Test 20

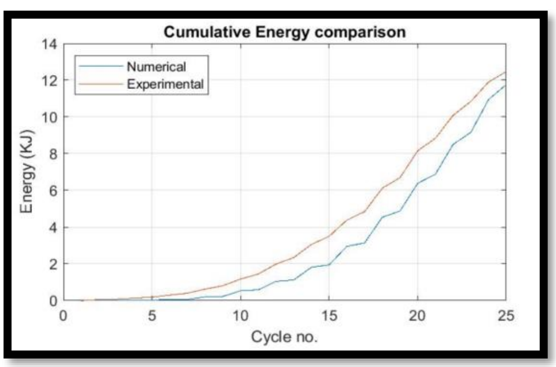

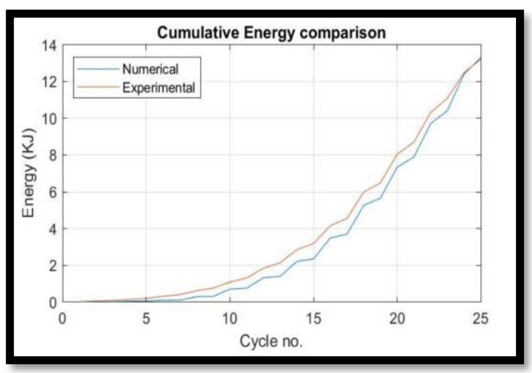

Figure 3.5.2.3 : Comparison of numerical and experimental cumulative energy dissipated

3.6. Group Models

Certain groups for the infilled façade were identified in order to reduce the dependence of numerical models on experimental data for similar configurations. This grouping was based on certain parameters like types of connection, stud spacing, number of panels, types of panels etc. The 8 different facades tested were grouped into 5 groups. The hysteretic characteristics of the group model are obtained by taking the mean of the backbone curve and the dependent cyclic parameters of pinching4 material of the configurations within the group. This ‘group model’ can simulate the response of all the models present in that certain group. The figure below shows the backbone of group models.

Figure 3.6: Backbone Curves of Group Models.

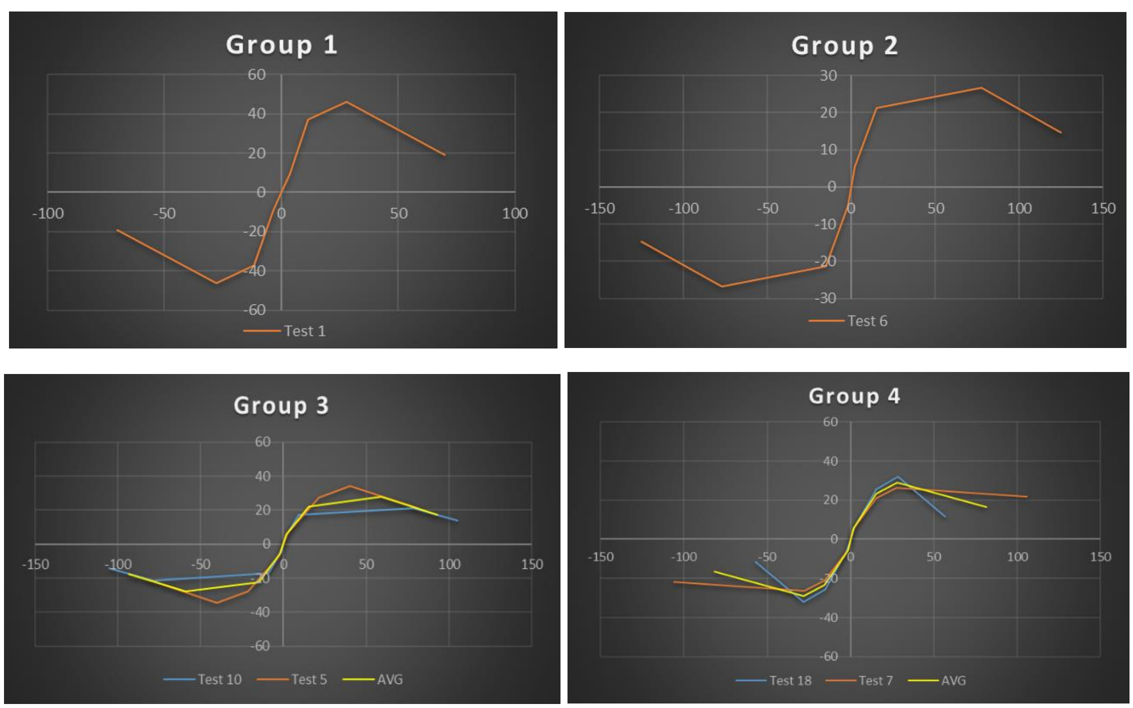

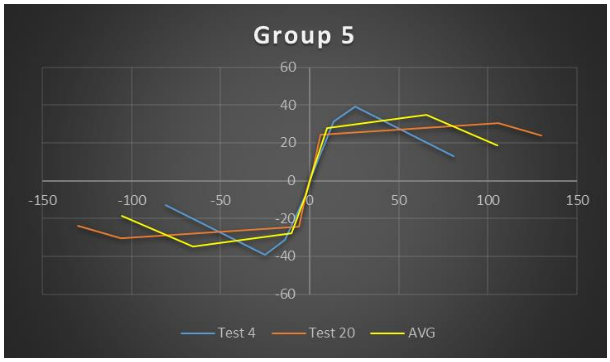

Table 3: Cyclic Parameters of Group Models.

GROUPS	CYCLIC LOAD																									
Cycles	1	2	3	4	5	6	7	8	9	10	11	12	13	14	15	16	17	18	19	20	21	22	23	24	25	26
Group 1																										
Test 1	3.1	3.1	4.4	4.4	6.4	6.4	9.3	9.3	13.3	13.3	19.3	19.6	27.8	28.1	40.4	40.9	57.7	57.9	81	81.5	106.5	106.8	131.3	131.4	156	156.3
Group 2																										
Test 6	3.2	3.2	4.4	4.7	6.7	6.7	9.3	9.3	13.6	13.8	19.8	20	28.5	28.6	40.7	41	57.7	57.9	80.9	81.2	105.9	106.2	130.8	131.1	155.8	155.9
Group 3																										
Test 5	3.2	3.2	4.7	4.7	6.7	6.7	9.3	9.3	13.3	13.4	19.5	19.6	28	28.1	40.3	40.7	57.4	57.7	81.2	81.5	106.3	106.7	131.1	131.3		
Test 10	3.6	3.6	4.9	5.2	7.2	7.2	10.3	10.3	14.3	14.3	20.3	20.3	28.8	29	41	41.2	57.9	58	81.2	81.4	106	106.2	130.7	130.9	155.4	155.6
Avg	3.4	3.4	4.8	4.95	6.95	6.95	9.8	9.8	13.8	13.85	19.9	19.95	28.4	28.55	40.65	40.95	57.65	57.85	81.2	81.45	106.15	106.45	130.9	131.1		
Group 4																										
Test 7	3.5	3.5	4.9	4.9	6.9	6.9	9.8	9.8	13.8	13.8	20.2	20.2	28.6	28.8	40.7	41.1	57.5	57.9	80.9	81.4	105.7	106.2	130.7	130.9	155.5	155.9
Test 18	3.2	3.2	4.4	4.4	6.4	6.4	9.3	9.3	13.3	13.3	19.6	19.6	28	28.1	40.5	40.7	57.4	57.9	80.9	81						
Avg	3.35	3.35	4.65	4.65	6.65	6.65	9.55	9.55	13.55	13.55	19.9	19.9	28.3	28.45	40.6	40.9	57.45	57.9	80.9	81.2						
Group 5																										
Test 4	3.2	3.2	4.4	4.7	6.7	6.7	9.3	9.3	13.6	13.8	19.8	20	28.5	28.6	40.7	41	57.7	57.9	80.9	81.2	105.9	106.2	130.8	131.1	155.8	155.9
Test20	3.5	3.5	4.9	4.9	6.9	6.9	9.8	9.8	13.8	13.8	20	20.2	28.6	28.8	40.7	41.1	57.5	57.9	80.9	81.4	105.7	106.2	130.7	130.9	155.5	155.9
Avg	3.35	3.35	4.65	4.8	6.8	6.8	9.55	9.55	13.7	13.8	19.9	20.1	28.55	28.7	40.7	41.05	57.6	57.9	80.9	81.3	105.8	106.2	130.75	131	155.65	155.9

3.7. Building Model

For this study a G+5 X-CBF steel frame building has been used. The building was first modeled in ETABS and was used to get the steel sections required. The building model is shown in the figure below

Figure 3.7: ETABS Building Model

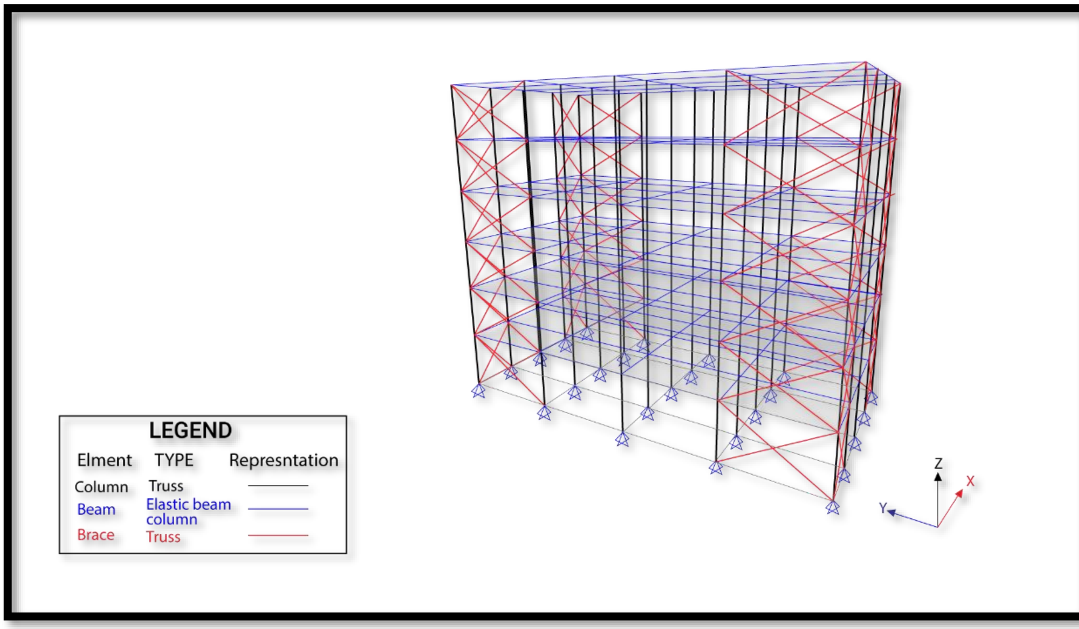

The strongest sections were extracted from the ETABS model and then used in the OpenSEES model.

Table 4: Section Properties

Properties	Column	Beam	Brace	
Section	W14x426	W12x132	L6x6x1/2	L8x6x7/16
Grade of Steel	50	50	50	50
Type of element	Truss	Elastic Beam Column	Truss	Truss

3.8. OpenSEES Model

The design building was then modelled in OpenSEES. The model was 3D in nature and had 6 degrees of freedom. The software does not have a GUI, therefore the building was modelled by coding. The software used to write the code was NotePad++ and the extention of all the files was .tcl .

1. Model Description : This includes all the basic information like story heights, bay widths and the properties of the elements involved
2. Grid Nodes : A total of 175 grid nodes were required to form the whole building. The nodes were definde based on the dimensions defined in model description.
3. Elements : All the information regarding the elements and their respective properties and type of material used for them was defined.
4. Façade : The details of all the neccessary information regarding the facades ie zerolength elements and truss elements were included in the model.

The building was first modelled without including facades in it. After running the pushover analysis and achieving the desired pushover curve, the facades were then added and the same pushover analysis was performed. The figure below shows the two models generated.

Figure 3.8.1: Building model without façade

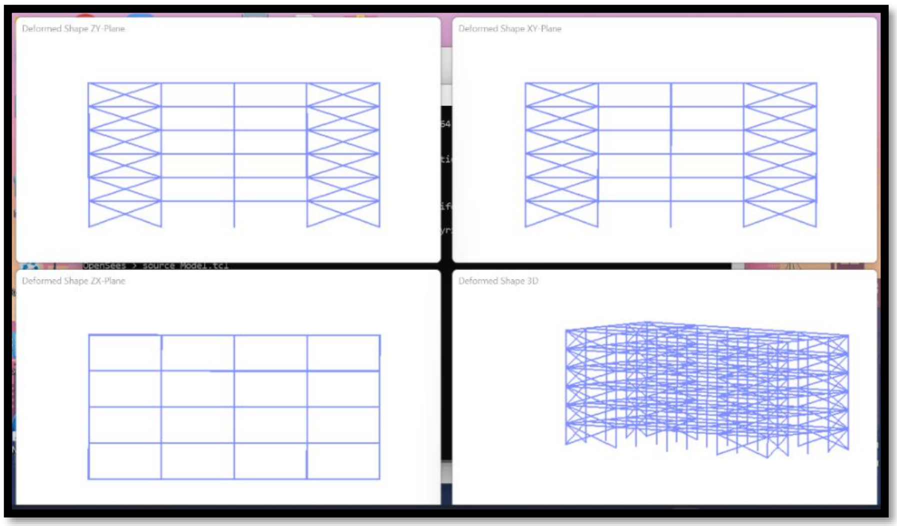

Figure 3.8.2: Building Model with façade

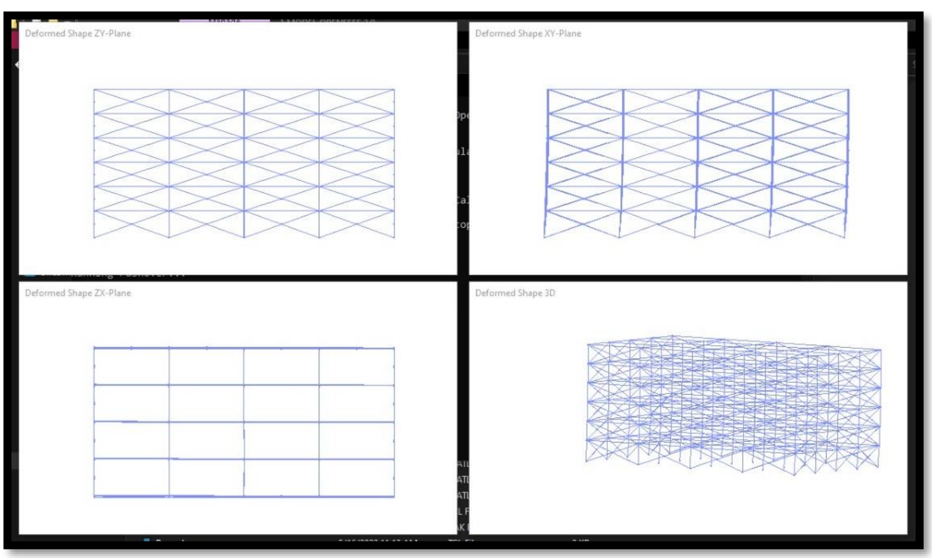

For beams and columns, Elastic material was used. For the Bracing elements the material used was Elastic Perfectly Plastic. The beams were modelled as elasticBeamColumn elements and the columns and braces were modelled as truss elements. For columns and bracing MinMax material was used in order to incorporate the buckling of columns and bracing elements. MinMax material has 2 main parameters, minStrain and maxStrain which are the values of strains at failure. These values were calculated by using the buckling stress of the respective columns.

For the truss elements connecting the zerolength spring element with the surrounding structural members, Elastic material was used and they were modelled as truss elements.The zerolength element was made of Pinching4 material. The zerolength spring element was allowed to translate in a single axis only, therefore the command equalDOF was used which does not allow the truss element connected to the zerolength spring element to move in any other axis than the one in which zerolength spring element translates in. If there is any movement in a plane other than the one in which the zerlength speing element translates in, the model analysis fails as it does not know about the element's behaviour in such a scenario. This had to be done for each of the 96 façade present in the bulding.

The pushover annalysis was based on lateral loadings that were calculated on the basis of floor weigths and the respective story heights. These loadings were then applied to their corressponding floor nodes. A portion of the code for running pushover is shown below.

Figure 3.8.3: Coding for Pushover analysis

```
set WBuilding 21400;
set NBays 4;
set W1H1 [expr $F1W*$H1];
set W2H2 [expr $F2W*$H2];
set W3H3 [expr $F3W*$H4];
set W4H4 [expr $F4W*$H4];
set W5H5 [expr $F5W*$H5];
set W6H6 [expr $F6W*$H6];
set sumWiHi [expr $W1H1 + $W2H2 + $W3H3 + $W4H4 + $W5H5 + $W6H6];
set lat1 [expr 1.0/($NBays+1.0) * $WBuilding * $W1H1/$sumWiHi];     # force on each frame node in Floor 1
set lat2 [expr 1.0/($NBays+1.0) * $WBuilding * $W2H2/$sumWiHi];     # force on each frame node in Floor 2
set lat3 [expr 1.0/($NBays+1.0) * $WBuilding * $W3H3/$sumWiHi];     # force on each frame node in Floor 3
set lat4 [expr 1.0/($NBays+1.0) * $WBuilding * $W4H4/$sumWiHi];     # force on each frame node in Floor 4
set lat5 [expr 1.0/($NBays+1.0) * $WBuilding * $W5H5/$sumWiHi];     # force on each frame node in Floor 5
set lat6 [expr 1.0/($NBays+1.0) * $WBuilding * $W6H6/$sumWiHi];     # force on each frame node in Floor 6

pattern Plain 2 Linear {
                load 211 $lat1 0.0 0.0 0.0 0.0 0.0;
                load 215 $lat1 0.0 0.0 0.0 0.0 0.0;

                load 311 $lat2 0.0 0.0 0.0 0.0 0.0;
                load 315 $lat2 0.0 0.0 0.0 0.0 0.0;

                load 411 $lat3 0.0 0.0 0.0 0.0 0.0;
                load 415 $lat3 0.0 0.0 0.0 0.0 0.0;

                load 511 $lat4 0.0 0.0 0.0 0.0 0.0;
                load 515 $lat4 0.0 0.0 0.0 0.0 0.0;

                load 611 $lat5 0.0 0.0 0.0 0.0 0.0;
                load 615 $lat5 0.0 0.0 0.0 0.0 0.0;

                load 711 $lat6 0.0 0.0 0.0 0.0 0.0;
                load 715 $lat6 0.0 0.0 0.0 0.0 0.0;
```

The same pushover analysis was run for the two available models, one with façade and one without façade. The pushover curves of building model and their comparison is shown below.

Figure 3.8.4: Pushover for building without façade.

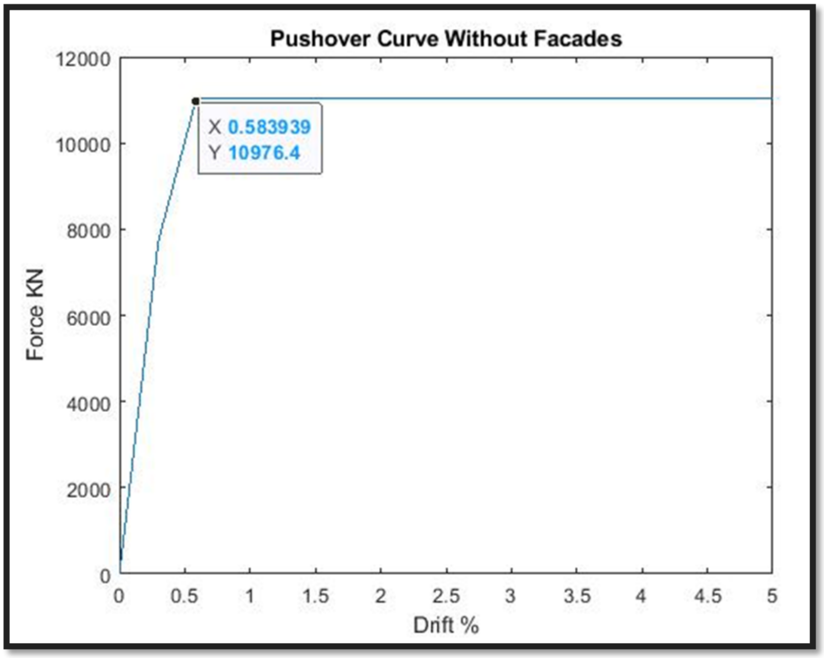

Figure 3.8.5 : Comparison of pushover curves of both building models.

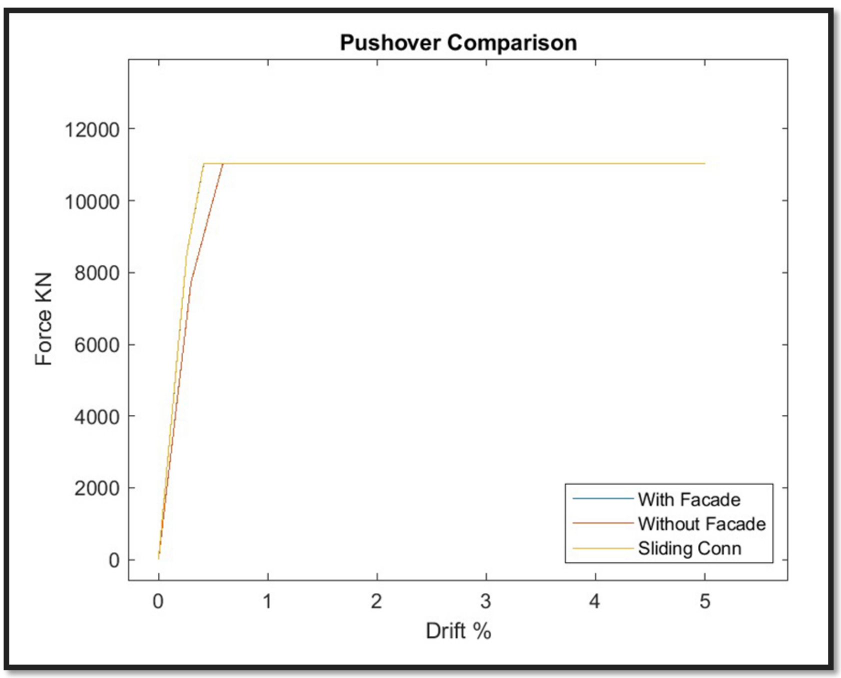

CHAPTER FOUR

4. RESULTS AND CONCLUSION

This study describes the methodology and effects of a quantification study at the contribution of non-structural LGS gypsum Façade models to the structural response of CFS buildings.

Previous experimental research has concluded that the design of CFS structures as per current AISI requirements results in a secure but over-conservative structure. This conservatism is introduced in by means of the unavoidable addition of non-structural elements inside the structure. Including all of the non-structural elements within the model is time-consuming from both modeling and analysis views.

This study is conducted to apprehend the effect of non-structural facades on the nonlinear response of CFS buildings. To this end, a systematic quantitative methodology is adopted in this study by analyzing 8 numerical models of outdoor facades and the results are given. The energy comparison between the numerical and experimental model is also shown. The rf and rd values are adjusted in such a way so as to avoid the over-estimation of numerical models compared to the experimental results.

After generating the backbone curves, the models have been grouped (5 groups) according to the similarity in backbones. Each group can now be tested in a building model to see which configuration has the most positive effect in resisting loads.

After grouping the models, a building (G+5 storey), whose sections were chosen using Etabs, has been modelled using OpenSEES. It is then subjected to a dynamic/pushover analysis with and without facades and the pushover curves (shown below) were observed.

The following conclusions were made from the pushover curves:

- It can be seen, from the given graph, that the model with infilled facades have a slightly lesser values for drift/displacement for the same amount of force as compared to the model having no infilled facades.

Figure 4.1.1: Pushover Comparison

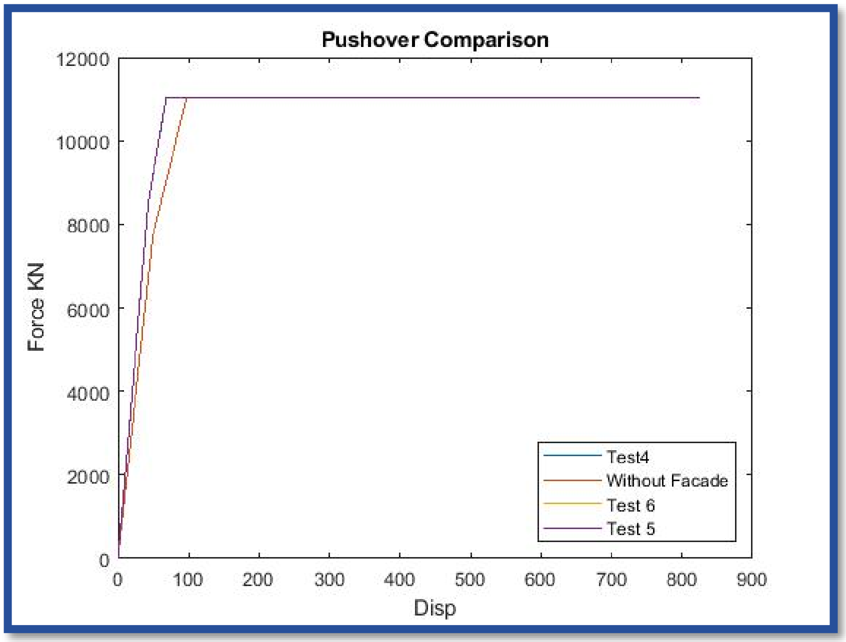

- The model consisting of infilled facades enter the non-linear range at a stage later than the model having no facades in it. (Points, as shown below in the graphs, show the difference)

Figure 4.1.2: Numerical Comparison

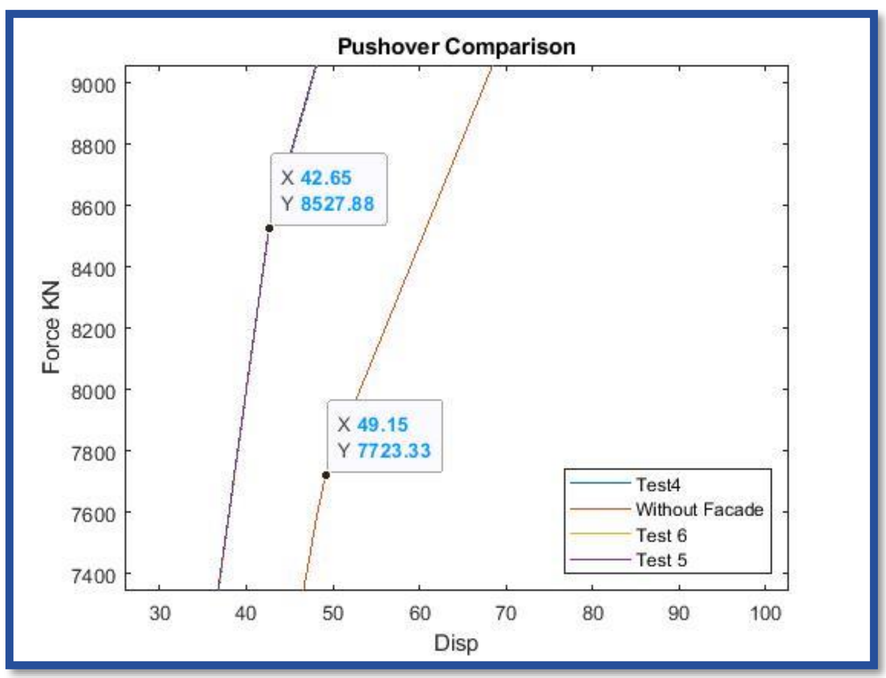

- This shows that the addition of infilled facades results in **increase in stiffness** of the structure
- This also helps in reducing the time period of the structure therefore increasing the seismic performance of the structure.
- The difference in the curves of different infilled façade models is not that much. They have a minor difference

- In the following graph, we can say that infilled façade used in test 5 has the best performance as it reaches the non-linear range at a slightly later stage compared to the other facades.

Figure 4.1.3: Comparison of pushover of different Façade configurations

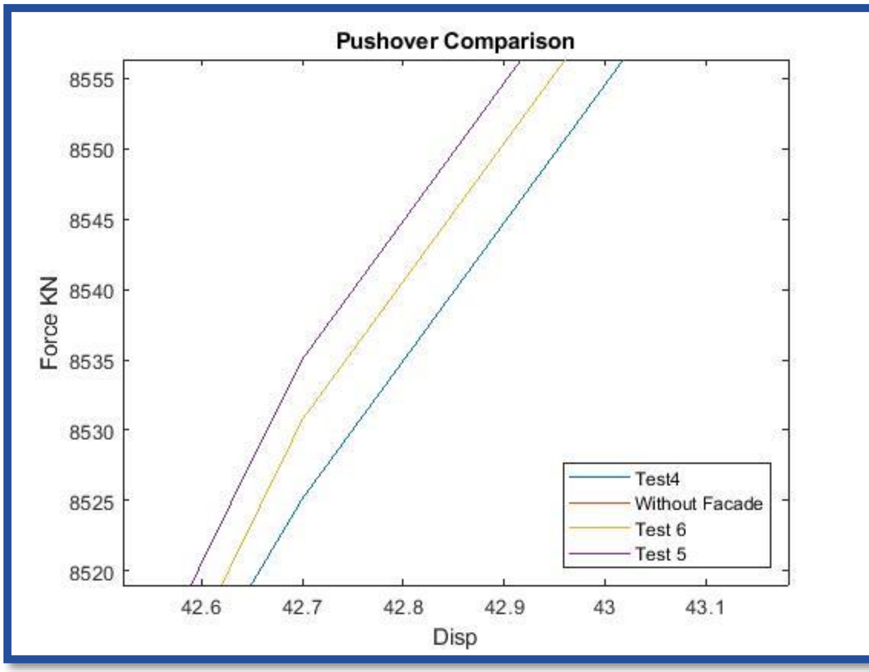

5. RECOMMENDATIONS

In our scope of research, the effect of façade on structural response of the whole building was studied and we could see, from the results, that there was a slight increase in the stiffness of the building when it was analyzed in OpenSEES including facades.

It is recommended that the response of the building at member level should be studied by using Finite Element Analysis (FEM) method. This would help us to better under the behavior of the building under seismic loads.

6. REFERENCES

1. Atkinson, G. M. (2009). Earthquake time histories compatible with the 2005 *National building code of Canada* uniform hazard spectrum. *Canadian Journal of Civil Engineering*, *36*(6), 991–1000. https://doi.org/10.1139/L09-044
2. Fiorino, L., Shakeel, S., Macillo, V., & Landolfo, R. (2017). Behaviour factor (q) evaluation the CFS braced structures according to FEMA P695. *Journal of Constructional Steel Research*, *138*, 324–339. https://doi.org/10.1016/j.jcsr.2017.07.014
3. Iuorio, O., Macillo, V., Terracciano, M. T., Pali, T., Fiorino, L., & Landolfo, R. (2014). Seismic response of Cfs strap-braced stud walls: Experimental investigation. *Thin-Walled Structures*, *85*, 466–480. https://doi.org/10.1016/j.tws.2014.09.008
4. Jenkins, C., Soroushian, S., Rahmanishamsi, E., & Maragakis, E. M. (2016). Experimental fragility analysis of cold-formed steel-framed partition wall systems. *Thin-Walled Structures*, *103*, 115–127. https://doi.org/10.1016/j.tws.2016.02.015
5. Källsner, B., & Girhammar, U. A. (2009). Plastic models for analysis of fully anchored light-frame timber shear walls. *Engineering Structures*, *31*(9), 2171–2181. https://doi.org/10.1016/j.engstruct.2009.03.023
6. Landolfo, R. (2019). Lightweight steel framed systems in seismic areas: Current achievements and future challenges. *Thin-Walled Structures*, *140*, 114–131. https://doi.org/10.1016/j.tws.2019.03.039
7. Landolfo, R., Shakeel, S., & Fiorino, L. (2022a). Lightweight steel systems: Proposal and validation of seismic design rules for second generation of Eurocode 8. *Thin-Walled Structures*, *172*, 108826. https://doi.org/10.1016/j.tws.2021.108826
8. Landolfo, R., Shakeel, S., & Fiorino, L. (2022b). Lightweight steel systems: Proposal and validation of seismic design rules for second generation of Eurocode 8. *Thin-Walled Structures*, *172*, 108826. https://doi.org/10.1016/j.tws.2021.108826
9. Lee, T.-H., Kato, M., Matsumiya, T., Suita, K., & Nakashima, M. (2007). Seismic performance evaluation of non-structural components: Drywall partitions. *Earthquake Engineering & Structural Dynamics*, *36*(3), 367–382. https://doi.org/10.1002/eqe.638
10. Liu, P., Peterman, K. D., & Schafer, B. W. (2014). Impact of construction details on OSB-sheathed cold-formed steel framed shear walls. *Journal of Constructional Steel Research*, *101*, 114–123. https://doi.org/10.1016/j.jcsr.2014.05.003
11. Magliulo, G., Petrone, C., Capozzi, V., Maddaloni, G., Lopez, P., & Manfredi, G. (2014). Seismic performance evaluation of plasterboard partitions via shake table tests. *Bulletin of Earthquake Engineering*, *12*(4), 1657–1677. https://doi.org/10.1007/s10518-013-9567-8
12. McCutcheon, W. J. (1985). Racking Deformations in Wood Shear Walls. *Journal of Structural Engineering*, *111*(2), 257–269. https://doi.org/10.1061/(ASCE)0733-9445(1985)111:2(257)
13. Pali, T., Macillo, V., Terracciano, M. T., Bucciero, B., Fiorino, L., & Landolfo, R. (2018). In-plane quasi-static cyclic tests of nonstructural lightweight steel drywall partitions for seismic performance evaluation. *Earthquake Engineering & Structural Dynamics*, *47*(6), 1566–1588. https://doi.org/10.1002/eqe.3031
14. Pali, T., Shakeel, S., & Landolfo, R. (2019). Experimental investigation on the seismic performance of LWS drywall architectural non-structural elements. *Proceedings of 4SPONSE Workshop*. https://doi.org/10.7414/4sponse.ID.40
15. Peterman, K. D., Nakata, N., & Schafer, B. W. (n.d.). *Cyclic Behavior of Cold-Formed Steel Stud-to-Sheathing Connections*. 8.

16. Peterman, K. D., Nakata, N., & Schafer, B. W. (2014). Hysteretic characterization of cold-formed steel stud-to-sheathing connections. *Journal of Constructional Steel Research*, *101*, 254–264. https://doi.org/10.1016/j.jcsr.2014.05.019
17. Peterman, K. D., Stehman, M. J. J., Madsen, R. L., Buonopane, S. G., Nakata, N., & Schafer, B. W. (2016). Experimental Seismic Response of a Full-Scale Cold-Formed Steel-Framed Building. II: Subsystem-Level Response. *Journal of Structural Engineering*, *142*(12), 04016128. https://doi.org/10.1061/(ASCE)ST.1943-541X.0001578
18. Petrone, C., Magliulo, G., Lopez, P., & Manfredi, G. (2015). Seismic fragility of plasterboard partitions via in-plane quasi-static tests: Seismic Fragility of Plasterboard Partitions. *Earthquake Engineering & Structural Dynamics*, *44*(14), 2589–2606. https://doi.org/10.1002/eqe.2600
19. Restrepo, J. I., & Bersofsky, A. M. (2011). Performance characteristics of light gage steel stud partition walls. *Thin-Walled Structures*, *49*(2), 317–324. https://doi.org/10.1016/j.tws.2010.10.001
20. Restrepo, JoséI., & Lang, A. F. (2011). Study of Loading Protocols in Light-Gauge Stud Partition Walls. *Earthquake Spectra*, *27*(4), 1169–1185. https://doi.org/10.1193/1.3651608
21. Retamales, R., Davies, R., Mosqueda, G., & Filiatrault, A. (2013). Experimental Seismic Fragility of Cold-Formed Steel Framed Gypsum Partition Walls. *Journal of Structural Engineering*, *139*(8), 1285–1293. https://doi.org/10.1061/(ASCE)ST.1943-541X.0000657
22. Shakeel, S., Fiorino, L., & Landolfo, R. (2020). Behavior factor evaluation of CFS wood sheathed shear walls according to FEMA P695 for Eurocodes. *Engineering Structures*, *221*, 111042. https://doi.org/10.1016/j.engstruct.2020.111042
23. Shakeel, S., Landolfo, R., & Fiorino, L. (2019). Behaviour factor evaluation of CFS shear walls with gypsum board sheathing according to FEMA P695 for Eurocodes. *Thin-Walled Structures*, *141*, 194–207. https://doi.org/10.1016/j.tws.2019.04.017
24. Shamim, I., DaBreo, J., & Rogers, C. A. (2013). Dynamic Testing of Single- and Double-Story Steel-Sheathed Cold-Formed Steel-Framed Shear Walls. *Journal of Structural Engineering*, *139*(5), 807–817. https://doi.org/10.1061/(ASCE)ST.1943-541X.0000594
25. Shamim, I., & Rogers, C. A. (2013). Steel sheathed/CFS framed shear walls under dynamic loading: Numerical modelling and calibration. *Thin-Walled Structures*, *71*, 57–71. https://doi.org/10.1016/j.tws.2013.05.007
26. Shamim, I., & Rogers, C. A. (2015). Numerical evaluation: AISI S400 steel-sheathed CFS framed shear wall seismic design method. *Thin-Walled Structures*, *95*, 48–59. https://doi.org/10.1016/j.tws.2015.06.011
27. Swensen, S., Deierlein, G. G., & Miranda, E. (2016). Behavior of Screw and Adhesive Connections to Gypsum Wallboard in Wood and Cold-Formed Steel-Framed Wallettes. *Journal of Structural Engineering*, *142*(4). https://doi.org/10.1061/(ASCE)ST.1943-541X.0001307
28. Tasligedik, A. S., Pampanin, S., & Palermo, A. (2015). Low damage seismic solutions for non-structural drywall partitions. *Bulletin of Earthquake Engineering*, *13*(4), 1029–1050. https://doi.org/10.1007/s10518-014-9654-5
29. Vitale, P., Spagnuolo, A., Lubritto, C., & Arena, U. (2018). Environmental performances of residential buildings with a structure in cold formed steel or reinforced concrete. *Journal of Cleaner Production*, *189*, 839–852. https://doi.org/10.1016/j.jclepro.2018.04.088
30. Wang, X., Pantoli, E., Hutchinson, T. C., Restrepo, J. I., Wood, R. L., Hoehler, M. S., Grzesik, P., & Sesma, F. H. (2015). Seismic Performance of Cold-Formed Steel Wall Systems in a Full-Scale Building. *Journal of Structural Engineering*, *141*(10), 04015014. https://doi.org/10.1061/(ASCE)ST.1943-541X.0001245

31. Wood, R. L., & Hutchinson, T. C. (2014). Design-Oriented Model for Capturing the In-Plane Seismic Response of Partition Walls. *Journal of Structural Engineering*, *140*(6), 04014023. https://doi.org/10.1061/(ASCE)ST.1943-541X.0000899
32. Yanagi, N., & Yu, C. (2014). Effective Strip Method for the Design of Cold-Formed Steel Framed Shear Wall with Steel Sheet Sheathing. *Journal of Structural Engineering*, *140*(4), 04013101. https://doi.org/10.1061/(ASCE)ST.1943-541X.0000870